



Article

Magnetized Activated Carbon Synthesized from Pomegranate Husk for Persulfate Activation and Degradation of 4-Chlorophenol from Wastewater

Sousan Hadi^{1,2}, Ensiyeh Taheri^{1,3}, Mohammad Mehdi Amin^{1,3}, Ali Fatehizadeh^{1,3,*} 
and Mohamed Khayet^{4,5,*} 

- ¹ Department of Environmental Health Engineering, School of Health, Isfahan University of Medical Sciences, Isfahan 8174673461, Iran; sousanhadi@gmail.com (S.H.); e_taheri@hlth.mui.ac.ir (E.T.); amin@hlth.mui.ac.ir (M.M.A.)
- ² Student Research Committee, School of Health, Isfahan University of Medical Sciences, Isfahan 8174673461, Iran
- ³ Environment Research Center, Research Institute for Primordial Prevention of Non-Communicable Disease, Isfahan University of Medical Sciences, Isfahan 8174673461, Iran
- ⁴ Department of Structure of Matter, Thermal Physics and Electronics, Faculty of Physics, University Complutense of Madrid, 28040 Avda. Complutense s/n, Madrid, Spain
- ⁵ Madrid Institute for Advanced Studies of Water (IMDEA Water Institute), Avda. Punto Com n° 2, 28805 Alcalá de Henares, Madrid, Spain
- * Correspondence: a.fatehizadeh@hlth.mui.ac.ir (A.F.); khayetm@fis.ucm.es (M.K.)



Citation: Hadi, S.; Taheri, E.; Amin, M.M.; Fatehizadeh, A.; Khayet, M. Magnetized Activated Carbon Synthesized from Pomegranate Husk for Persulfate Activation and Degradation of 4-Chlorophenol from Wastewater. *Appl. Sci.* **2022**, *12*, 1611. <https://doi.org/10.3390/app12031611>

Academic Editor: Alberto Milani

Received: 25 December 2021

Accepted: 31 January 2022

Published: 3 February 2022

Publisher's Note: MDPI stays neutral with regard to jurisdictional claims in published maps and institutional affiliations.



Copyright: © 2022 by the authors. Licensee MDPI, Basel, Switzerland. This article is an open access article distributed under the terms and conditions of the Creative Commons Attribution (CC BY) license (<https://creativecommons.org/licenses/by/4.0/>).

Abstract: The compound 4-chlorophenol (4-CP) is known to be a highly toxic compound having harmful effects on human health and the environment. To date, the removal of 4-CP by advanced oxidation processes (AOPs) has attracted tremendous attentions. The persulfate-based AOPs show higher oxidation, better selectivity, wider pH range, and no secondary pollution compared to the traditional Fenton-based AOPs. Carbon materials with low cost and chemical stability are useful for the activation of persulfate (PS) to produce reactive species. Herein, we magnetized activated carbon synthesized from pomegranate husk (MPHAC). By using 4-CP as a model organic pollutant, tests of the activation of PS via MPHAC for the removal of 4-CP were performed. Batch processes were carried out to study the influence of different parameters (initial solution pH, catalyst dose, PS dose, and initial 4-CP concentration) on the adsorption of 4-CP on PHAC with ferric oxide (Fe₃O₄-PHAC). The results show that under the obtained optimal conditions (MPHAC dose: 1250 mg/L, PS dose: 350 mg/L, solution pH 5, an initial 4-CP concentration of 100 mg/L, and a contact time of 60 min), a 4-CP removal factor of 99.5% was reached by the developed MPHAC/PS system. In addition, it was found that reusing MPHAC in five successive cycles is feasible because the catalyst in the last cycle kept exhibiting a high potential for 4-CP absorption, indicating the economically viable procedure. Therefore, this study provides a comprehensive understanding on the degradation of 4-CP by the magnetized activated carbon persulfate system.

Keywords: pomegranate husk; 4-chlorophenol; magnetized activated carbon; persulfate; reusability

1. Introduction

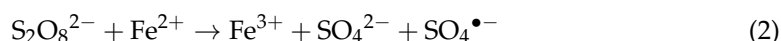
Today, the presence of organic pollutants in water is a major problem for human, animal and environmental health [1]. Chlorophenols (CPs) are organochlorides of phenol recognized as priority pollutants by the US Environmental Protection Agency. These compounds are very toxic and can cause many environmental problems due to their widespread use and release into the environment. These have been detected in surface water, groundwater, landfills, disposal sites and sludge produced in treatment plants [2]. CP are also found in bactericides, insecticides, herbicides, and fungicides [3]. In addition, CP can be produced as by-products during various processes, such as disinfection of drinking

water by chlorination process. The presence of CP in gases emitted from incinerators has been also identified [4]. Therefore, treatments of CP-contaminated wastewaters and CP removal before the discharge of wastewaters is essential.

Water and wastewater treatment methods are generally divided into three categories: physical, chemical, and biological. The physical methods include filtration, adsorption, flotation by air, extraction, flocculation, and sedimentation; the biological methods are aerobic (such as activated sludge) and anaerobic degradation; and the chemical methods include oxidation, ion exchange, and chemical precipitation [5–7]. These methods have disadvantages such as their high investment costs, high energy consumption, low operating speed, volatile emissions, toxic sludge production, complex equipment maintenance, etc. [8,9].

One of the most important applied methods to purify pollutants are the advanced oxidation processes (AOPs). In the AOPs methods, hydroxyl ($\bullet\text{OH}$), sulfate ($\text{SO}_4^{\bullet-}$), and superoxide ($\text{O}_2^{\bullet-}$) free radicals are produced, leading to the breakdown of pollutants and turning them into simple and low risk molecules. The advantages of this method include its non-toxicity, high oxidizing power of active radicals, no sludge production, short life of radicals, no corrosion of equipment, and its simple application [10]. Oxidants such as persulfate (PS) and hydrogen peroxide (H_2O_2) can be used. Persulfates are low-cost and environmentally stable oxidants that exist in both proxymonosulfate (PMS) and proxydisulfate (PDS). PS produces $\text{SO}_4^{\bullet-}$ radicals, which have a higher oxidation power ($E^0 = 2.5\text{--}3.1\text{ V}$) than hydroxyl radicals ($E^0 = 1.89\text{--}2.72\text{ V}$) [11]. These oxidants can be activated by different methods, such as heating, ultraviolet irradiation, and ultrasound (with different frequencies) [12,13]. In traditional AOPs like the Fenton process, the H_2O_2 and PS ions were applied with homogeneous iron salt as catalysts to produce $\bullet\text{OH}$ and $\text{SO}_4^{\bullet-}$ radicals. However, the main disadvantages of the Fenton process are the additional purification of iron ions, handling produced sludge, and effluents neutralization [14].

Nanoparticles are used in AOPs as nanocatalysts to increase the process efficiency. Methods such as filtration and centrifugation are often used to separate these nanoparticles, which have the disadvantages of being time-consuming and interrupting processes. To solve these problems, magnetic nanocatalysts can be used. These are synthesized by various methods such as sol-gel, heat decomposition, radiation, microwave, biological synthesis, and co-precipitation. The advantages of magnetic nanocatalysts include their easy synthesis, lack of toxicity, high chemical stability, and simple separation under a magnetic field without the use of chemicals and filtration. To make AOPs more efficient, magnetic nanocatalysts can be used in combination with various oxidants. Among all these procedures, the activation of PS by magnetic nanocatalysts is less complex and cheaper. It is carried out without the need for external energy [2]. Iron in magnetic nanocatalysts is one of the metals that is generally used to activate PS according to the following reactions [15].



One of the advantages of magnetic nanocatalysts is that the use of metal nanocatalysts is limited because of the drawbacks of the generated secondary pollution and environmental toxicity. This issue can be solved by bringing into contact the metal catalysts with carriers of a porous structure, such as graphene, activated carbon, zeolite or clay, after which the catalysts can be separated from water [16]. Because of its low cost, no electricity consumption and high efficiency, Fe-C micro-electrolysis has been widely used for the treatment of various wastewaters. In the Fe-C micro-electrolysis system, a large number of microscopic galvanic cells are formed between Fe and C, which produced highly active reactants like Fe(II) and H, and led to organic pollutants decomposition [17]. This method can increase the performance of catalysts by preventing the release of iron in solution and its adsorption at a given surface, thereby enhancing the removal efficiency of pollutants. For instance, activated carbon can be used as an iron support adsorbent [18]. It is considered

one of the most efficient adsorbents for removing organic compounds from wastewaters due to its porous structure and high adsorption capacity [19]. However, the use of activated carbon is limited due to its high cost, and agricultural wastes have been proposed for its production [20].

The pomegranate was cultivated in various countries including Iran, China, India, Greece, and Spain [21,22]. Pomegranates contain antioxidants and are consumed in large quantities due to their positive effects on human health [23,24] and antimicrobial properties [25]. Pomegranate husk (PH) is always treated as waste and is thrown in the trash. Since pomegranate husk contains organic acids, proteins, sugars, as well as large phenolic compounds, it can serve as a carbon precursor for the manufacture of carbon-based materials. In addition, as a result, the proper functioning of the pomegranate husk surface enhances the performance of carbon materials [21,26].

The aim of this study is to investigate the simultaneous adsorption and degradation of 4-chlorophenol (4-CP) by magnetized activated carbon synthesized from pomegranate husk (MPHAC) by the chemical activation method and surface coating of iron oxide particles (Fe_3O_4) for PS activation. 4-CP was selected as a model contaminant from wastewater because of its high toxicity and hard biodegradability. We used the MPHAC/PS system to remove 4-CP from water as it involves simultaneous adsorption and degradation processes to achieve a high 4-CP removal. The optimal conditions for 4-CP removal from water by the MPHAC/PS system were determined, its reusability was studied, and a possible mechanism and pathway of 4-CP removal is proposed.

2. Material and Methods

2.1. MPHAC Synthesis

To prepare MPHAC, collected pomegranate husk (PH) from a local market was first washed many times with deionized water and subsequently dried at 105 °C and ground. Then, 100 g of PH was added to 50 mL of ZnCl_2 aqueous solution (3M), and mixed under a temperature of 70–80 °C. The resulting paste was dried for 4 h at 105 °C in a furnace, and then the dried paste was transferred to a stainless-steel reactor and heated from room temperature to 600 °C at 10 °C/min for 30 min under the N_2 flux of 150 mL/min. Then, 10.0 g of carbonized material and 200 mL of HCl (6 M) were placed in a 500 mL boiling flask and the mixture was stirred on a magnetic stirrer and reflux for 2 h at 70–80 °C. The slurry was cooled down and filtered, washed with deionized water several times, milled, and finally, sieved. For PHAC magnetization, 2 mM $\text{FeCl}_3 \cdot 6\text{H}_2\text{O}$ and 1 mM $\text{FeCl}_2 \cdot 4\text{H}_2\text{O}$ were first mixed in 100 mL double distilled water and then 2 g of PHAC was added to the formed mixture. The obtained suspension was mixed under heating at 70 ± 2 °C and then ammonia solution was added drop-wise under N_2 atmosphere until the pH reached 11. After cooling, the synthesized MPHAC was repeatedly rinsed with double distilled water until its pH became neutral and finally dried at 105 °C.

2.2. MPHAC Characterization

Scanning electron microscope (SEM), X-ray powder diffraction (XRD), FTIR measurements, energy-dispersive X-ray spectroscopy (EDS), and vibrating sample magnetometry (VSM) was performed to determine the surface morphology, crystallization, the surface functional groups, chemical characterization, and magnetic properties of MPHAC, respectively. The surface area (S_{BET}) and pore size were determined by the Brunauer–Emmett–Teller (BET) and Barrett–Joyner–Halenda (BJH) methods. In addition, the drift method was employed to determine the pH of point of zero charge (pH_{PZC}) of MPHAC.

2.3. 4-CP Adsorption and Degradation Tests

The degradation tests of 4-CP were performed in 100 mL flasks containing 50 mL of the reaction solution formed by mixing PS and MPHAC. The solution was agitated at 180 rpm and 20 ± 3 °C for up to 90 min. Subsequently, the suspension was filtered and the residual concentration 4-CP was determined using an UV spectrophotometer

(DR 2000, Hach, Germany) at the wavelength 510 nm [2]. The effects of the solution pH (3–9), the MPHAC dose (250–1250 mg/L), the PS dose (50–350 mg/L), and the 4-CP initial concentration (100–250 mg/L) were investigated together with the MPHAC reusability. In order to perform the 4-CP extraction from MPHAC, 5 mL of acetonitrile/methanol (1/1, *v/v*) was mixed with the MPHAC sample for 2 h under 180 rpm, and finally dissolved with 5 mL of methanol for 4-CP detection.

To determine the 4-CP distribution in the aqueous phase (A_1) and solid phase (A_2), Equations (3) and (4) were employed.

$$A_1 = C_{aqueous} \times V / C_0 \times V \quad (3)$$

$$A_2 = C_{MPHAC} \times M / C_0 \times V \quad (4)$$

where $C_{aqueous}$ is the 4-CP concentration in the aqueous phase (mg/L), C_{MPHAC} is the concentration of 4-CP adsorbed on the MPHAC (mg/g), C_0 is the initial 4-CP concentration in the aqueous solution (mg/L), V is the volume of the aqueous phase (L), and M is the MPHAC mass in the aqueous solution (g).

The following equations were used to calculate the degradation of 4-CP by PS, its adsorption by MPHAC, and its removal factor:

$$Degradation(\%) = [1 - (A_1 + A_2)] \times 100 \quad (5)$$

$$Removal \ factor \ (\%) = (1 - A_1) \times 100 \quad (6)$$

$$Adsorption(\%) = Removal(\%) - Degradation(\%) \quad (7)$$

3. Results and Discussion

3.1. Characteristics of MPHAC

The synthesized MPHAC was characterized by means of different techniques and the obtained results are shown in Figures 1 and 2. The obtained SEM images of MPHAC microstructure are displayed in Figure 1a,b. As can be seen, the synthesized MPHAC exhibits a rough surface with cracks and pores, together with aggregation having a mean size of 57.61 ± 8.65 nm. In order to determine the chemical composition of MPHAC, EDS analysis was carried out and the results are presented in Figure 1c. The MPHAC powder contains not only carbon (C) with the highest fraction (52.3 wt%), oxygen (O) with 35 wt%, and a very low fraction of sulfur (S, 0.1 wt%), but also a high proportion of the metal iron (Fe, 12 wt%) and a lower proportion of zinc (Zn, 0.7 wt%). Moreover, the MPHAC was characterized by FTIR to analyze its chemical structure and functional groups. The obtained FTIR spectrum is plotted in Figure 1d. The vibrations at 3423.8 cm^{-1} are assigned to the bands O-H stretch, while the band located at 2922.6 cm^{-1} corresponds to the C-H vibrations in methyl and methylene groups [2]. The peak band at 1623.3 cm^{-1} is related to the aromatic ring mode [27]. The C-H band is associated to the peak at 1388 cm^{-1} , while the C-O stretching of phenolic or carboxylate groups corresponds to the peak at 1086.9 cm^{-1} [27]. The band at 564.7 cm^{-1} is assigned to Fe-O vibration [28]. The C-H out-of-plane bending causes the band at 477.8 cm^{-1} [27]. Ben-Ali [29] reported that the functional groups of PH include hydroxylic groups, the aliphatic C-H group, C=O stretching of the carbonyl group, and C-O groups of carboxylic acid, alcoholic, phenolic, ether, and ester groups.

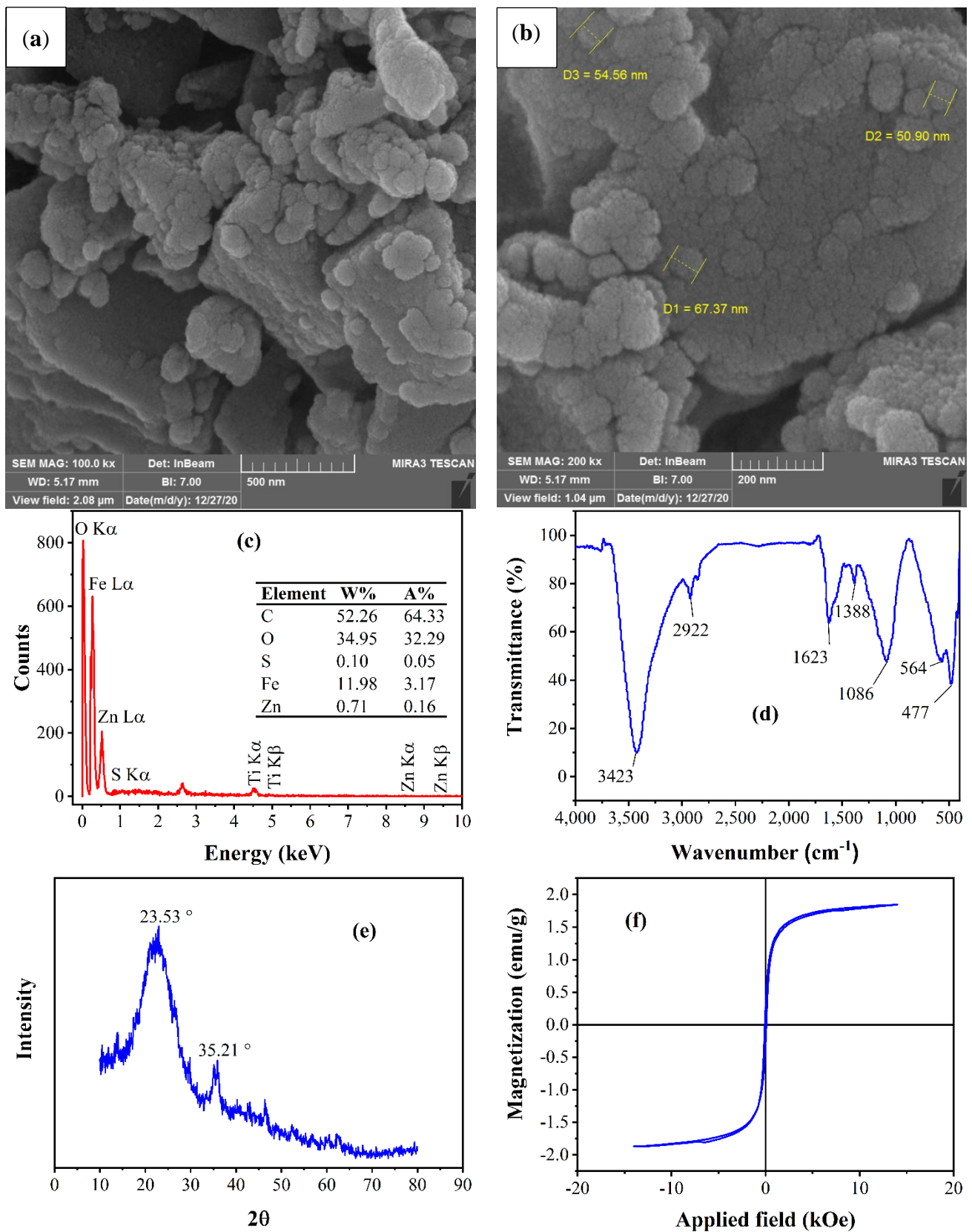


Figure 1. Characteristics of the synthesized MPHAC: Scanning electron microscopy (SEM) images (a) 500 nm magnitude (b), 200 nm magnitude, (c) Energy dispersive spectroscopy (EDS), (d) Fourier-transform infrared spectroscopy (FTIR), (e) X-ray diffraction (XRD), and (f) Vibrating sample magnetometry (VSM) patterns.

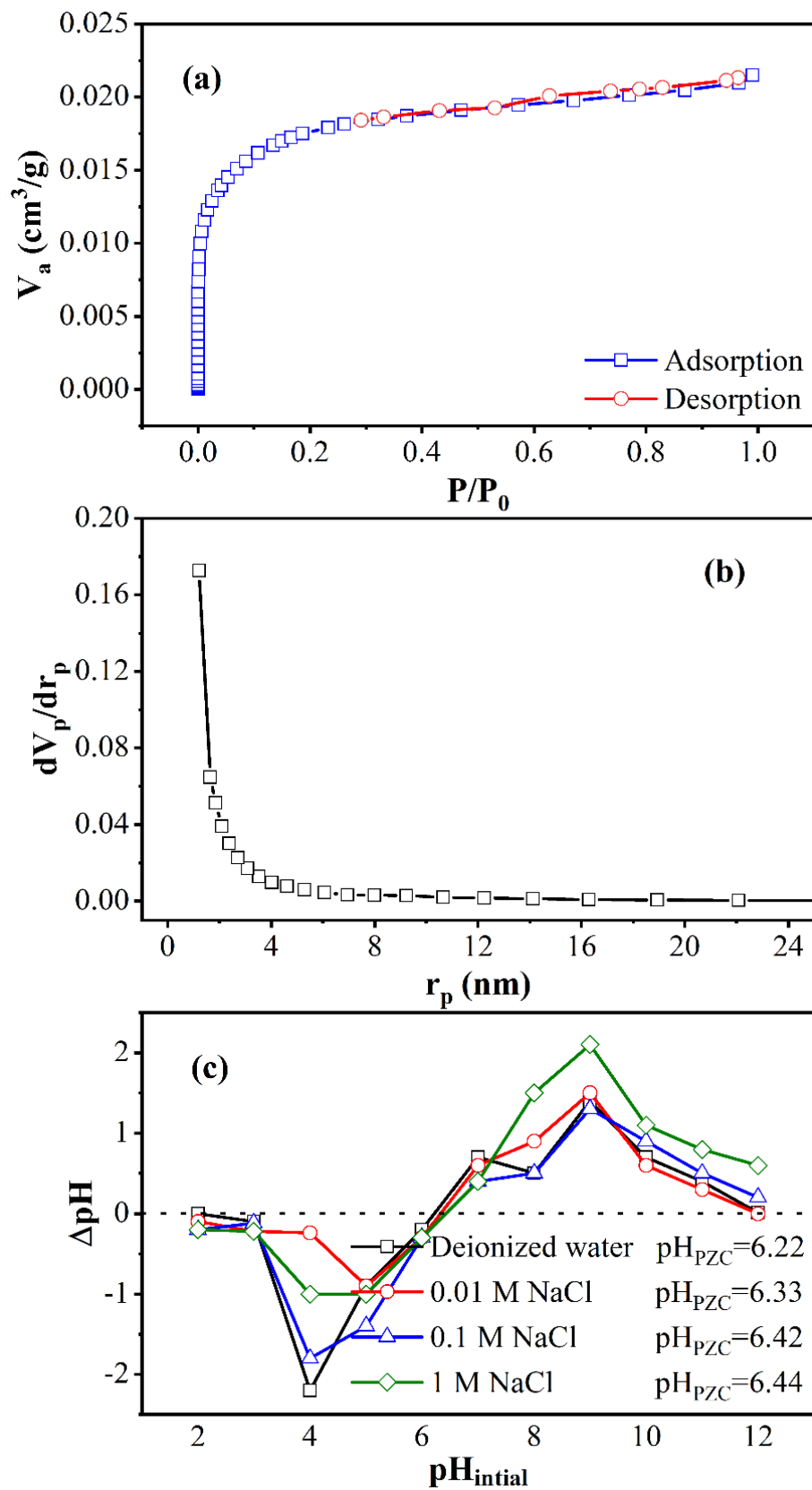


Figure 2. (a) Isotherms of N_2 adsorption and desorption, (b) distribution curve of pore size, and (c) effect of background electrolytes on pH_{PZC} of the synthesized MPHAC.

The diffractogram of the MPHAC shown in Figure 1e presents a broad peak at approximately $2\theta = 23.5^\circ$, corresponding to the plane, which is a feature of amorphous carbon. In addition, the peak of Fe_3O_4 particles was detected at $2\theta = 35.2^\circ$, confirming their presence in MPHAC. The magnetic property of MPHAC was also evaluated and displayed in Figure 1f. The saturation magnetization value, related to Fe_3O_4 formation in the matrix of MPHAC, was 1.75 emu/g. This is higher than the reported value for the magnetic separation by Du et al. [30], who synthesized magnetic activated carbon (AC/ Fe_3O_4) with iron contents of 5%, and reported that the saturation magnetization was 0.3 emu/g. In contrast, Khaledi et al. [31] reported that the saturation magnetization of magnetic activated carbon is around 13 emu/g at room temperature. All the above results confirmed the successful synthesis of MPHAC.

Figure 2a,b shows the BET isotherms of N_2 adsorption and desorption cycles, together with the porosity distribution of MPHAC. Based on the classification of IUPAC [32], the Type I adsorption isotherm was observed for MPHAC and the curve raised rapidly when the relative pressure P/P_0 was low, and then seemed to stabilize for higher P/P_0 values. When the relative pressure P/P_0 was lower than 0.1, the isothermal adsorption curve was related to the number of micropores [2,33]. The estimated specific total pore volume (V_{total}), specific surface area (S_{BET}), and mean pore diameter of the synthesized MPHAC were $0.75 \text{ cm}^3/\text{g}$, $1363.4 \text{ m}^2/\text{g}$ and 2.19 nm, respectively.

The variation of different background electrolytes on the pH_{PZC} is shown in Figure 2c for the MPHAC dose 200 mg/L. As can be seen, the registered pH_{PZC} value, 6.35 ± 0.1 , is independent on the background electrolyte, ranging from deionized water to 1M NaCl. This result agrees with those reported in previous studies [34,35].

3.2. Removal of 4-CP by MPHAC, PS and the Combined MPHAC/PS System

In order to clarify the synergistic effect of MPHAC and PS, a series of preliminary experiments were performed under the same conditions using MPHAC alone, PS alone, and the MPHAC/PS system. The obtained 4-CP removal factor is plotted in Figure 3 as a function of the contact time. It was found that PS alone was able to remove only 9.7 ± 0.5 of 4-CP at a reaction time of 90 min. This low removal factor is due to the low activation of PS. As mentioned earlier, PS needs activators such as UV light, heat, or transfer metals, to activate and produce sulfate radicals. When using PS alone, the 4-CP removal mechanism is attributed only to the degradation process, which is not very efficient due to the inactivation of PS. On the other hand, when using MPHAC alone, the adsorption process is the predominant process for 4-CP removal. In this case, due to the high adsorption capacity of the used catalyst, a higher removal factor of 4-CP up to $49.7 \pm 2.2\%$ was achieved at a reaction time of 90 min. However, the combined MPHAC/PS system exhibited the highest 4-CP removal factor, $79.1 \pm 3.5\%$, at a reaction time of 90 min. This system removes a high percentage of 4-CP from the beginning of the reaction, $47.8 \pm 2.4\%$ after 2 min, indicating that MPHAC is a highly efficient catalyst in the Fenton-like process. Simultaneous adsorption and degradation processes are involved in this system, resulting in an effective removal of 4-CP. The Fe_3O_4 particles on the catalyst surface lead to the activation of PS and the subsequent degradation process. As a result, the MPHAC/PS system was used in the following experiments and the optimized parameters for an efficient 4-CP removal were determined. Su et al. [36] prepared nano Fe^0 -loaded superfine powdered activated carbon for synergistic adsorption and PS activation to remove carbamazepine (CBZ) from aqueous solution. It was observed that CBZ could not be degraded by PS alone. However, a higher removal efficiency of CBZ was obtained for Fe^0 -loaded activated carbon in the presence of PS, suggesting that the removal efficiency was improved by adding PS to the reaction.

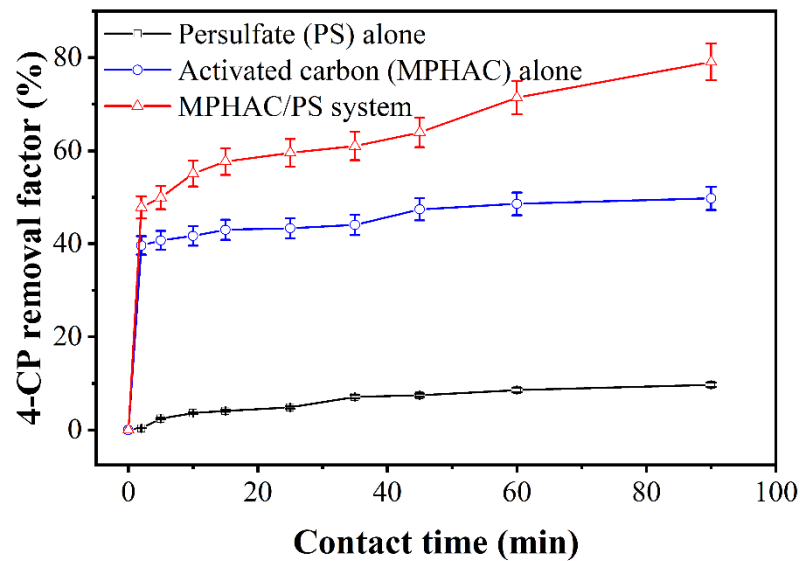


Figure 3. 4-CP removal factor of MPHAC, PS, and the combined MPHAC/PS system as a function of the reaction contact time (4-CP concentration: 150 mg/L; MPHAC dose: 250 mg/L; PS dose: 150 mg/L; and a solution pH of 7).

3.3. Factors Affecting the Removal of 4-CP by the Combined MPHAC/PS System

3.3.1. Effect of the Initial Solution pH on 4-CP Adsorption and Degradation

One of the most important and fundamental factors in advanced oxidation processes is the pH of the solution to be treated, because of its importance in the ionization of pollutants and oxidants, pollutant decomposition, catalyst surface structure, oxidant activity, and solubility [37]. For instance, it plays an important role on the activity of active species in the MPHAC/PS system, as shown in Figure 4, presenting both the adsorption and degradation of 4-CP at different pH values 3, 5, 7 and 9.

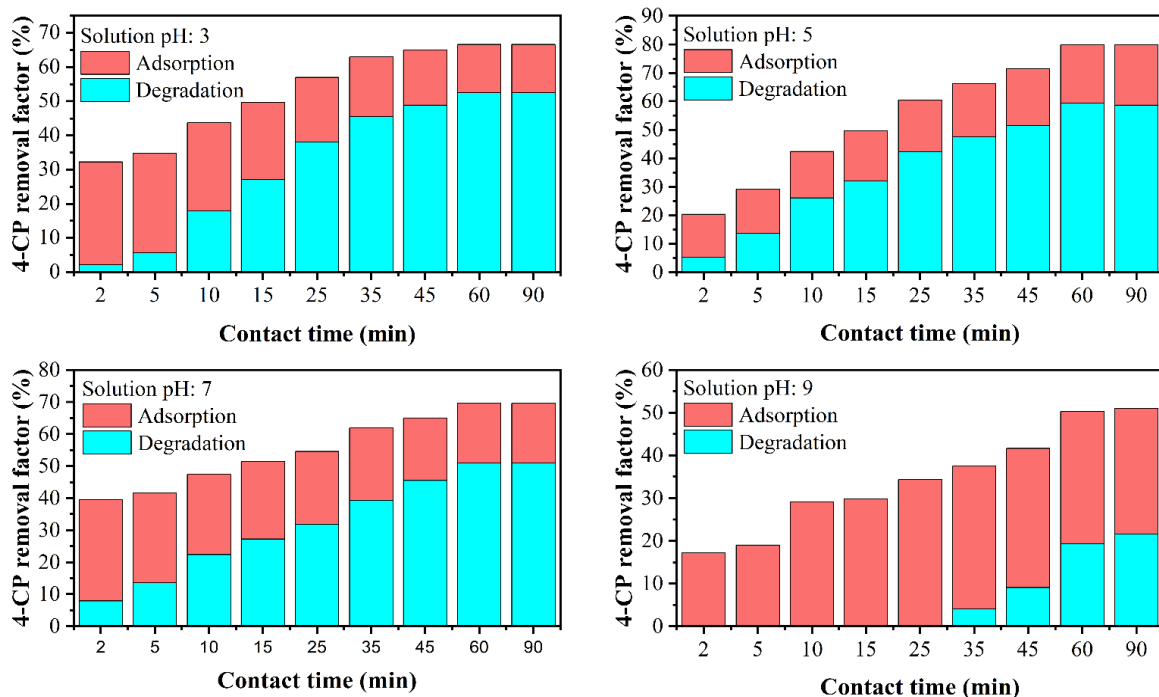


Figure 4. Effect of the initial solution pH on 4-CP removal factor using the MPHAC/PS system (initial 4-CP concentration: 100 mg/L; MPHAC dose: 150 mg/L; and PS dose: 150 mg/L).

As can be seen from Figure 4, in acidic conditions, the removal of 4-CP was higher than in alkaline conditions. The percentage of 4-CP removal decreased dramatically from 80 to 50%, as the initial pH increased from 5 to 9 due to the electrostatic attraction between the 4-CP molecules and the surface of MPHAC. It is necessary to know the pH_{PZC} of the catalyst and pK_a of 4-CP in order to analyze the observed different 4-CP removal factors of the MPHAC/PS system at different pH values. The obtained pH_{PZC} value of the synthesized MPHAC in this study was 6.35. When the pH of the solution is higher than 6.35 ($pH > pH_{PZC}$), the surface charge of the catalyst becomes negative, and at pH values below 6.35 ($pH < pH_{PZC}$), the surface load of the catalyst becomes positive [28]. On the other hand, taking into consideration that the 4-CP pK_a value is 4.7, 4-CP has a positive charge in acidic conditions ($pH < pK_a$), preventing the adsorption of 4-CP on the surface of the catalyst. According to the above description, the highest removal efficiency was observed when $pK_a < pH < pH_{PZC}$. In other words, in this pH range, 4-CP molecules have an anion form and are adsorbed on the surface of the catalyst having a positive charge. Moreover, the observed higher 4-CP removal factors in acidic solutions compared to alkaline solutions is attributed partly to the fact that in alkaline conditions, PS is repelled from the catalyst surface due to its anionic property, released in the solution, and its activation is stopped as consequence [38]. This phenomenon is noticeable at pH 9, confirming the decrease of the PS activity. The obtained results are in line with those reported by Liu et al. [39], who studied propachlor degradation by ferrous and copper ion activated PS, and reported that at basic pH conditions, the activation of PS decreased via copper hydrolysis. However, the findings were opposite to those of Chen et al. [40], who demonstrated that the combination of biochar and PS had relatively good activation efficacy of PS under a wide range of initial pH 4–9 values.

In addition to the effect of the initial pH value on the 4-CP adsorption and degradation processes of the MPHAC/PS system, the effect of the reaction time on the 4-CP removal process was investigated in order to understand the behavior of 4-CP adsorption and degradation along the contact reaction time. As shown in Figure 4, in all ranges of pH values, at the beginning of the reaction, the adsorption process dominated the 4-CP removal process. Then, over time, the degradation process becomes gradually dominant for all test pH values, except at the pH 9, in which the adsorption process is maintained to be higher than the degradation process. At the beginning of the reaction, PS does not have enough time to be activated and 4-CP removal often occurs by the adsorption process. However, over time, PS is adsorbed to the catalyst surface of the MPHAC and sulfate radicals are produced, inducing 4-CP degradation and enhancement of 4-CP removal [16]. As indicated previously, at pH 9, PS is repelled from the catalyst surface due to its anionic property and its activation is reduced, confirming that, for this pH value, adsorption is the predominant process for 4-CP removal.

3.3.2. Effect of MPHAC dose on 4-CP Adsorption and Degradation

In general, the catalyst plays an important role in removing pollutants from contaminated waters. Figure 5 shows the performance of the MPHAC/PS system at different doses of MPHAC for 4-CP removal. As it can be seen, the removal efficiency of 4-CP with different MPHAC doses 250, 750 and 1250 mg/L is 79.9, 83.6 and 94.7% at a reaction time of 90 min, respectively. The increase of the 4-CP removal with increasing MPHAC dose is due to the enhancement of the number of active sites on the catalyst surface, which increases the likelihood of adsorption and degradation of 4-CP.

With the increase of catalyst, the iron ions existing on the surface of the catalyst increase, leading to more activation of PS and production of more sulfate radicals [41]. Moreover, by increasing the amount of the catalyst, the adsorption process acquired a more effective role in 4-CP removal than the degradation process because the amount of PS is maintained constant for the different considered doses of the catalyst. In other words, although there are more active sites in higher catalyst doses in the MPHAC/PS system, not enough PS is present to produce sulfate radicals and the relative degradation process is

reduced [42]. These results are similar to the ones obtained by Rao et al. [43], who found that by applying an appropriate dose of the catalyst, 97.8% of reactive red M-3BE was removed after 20 min reaction time.

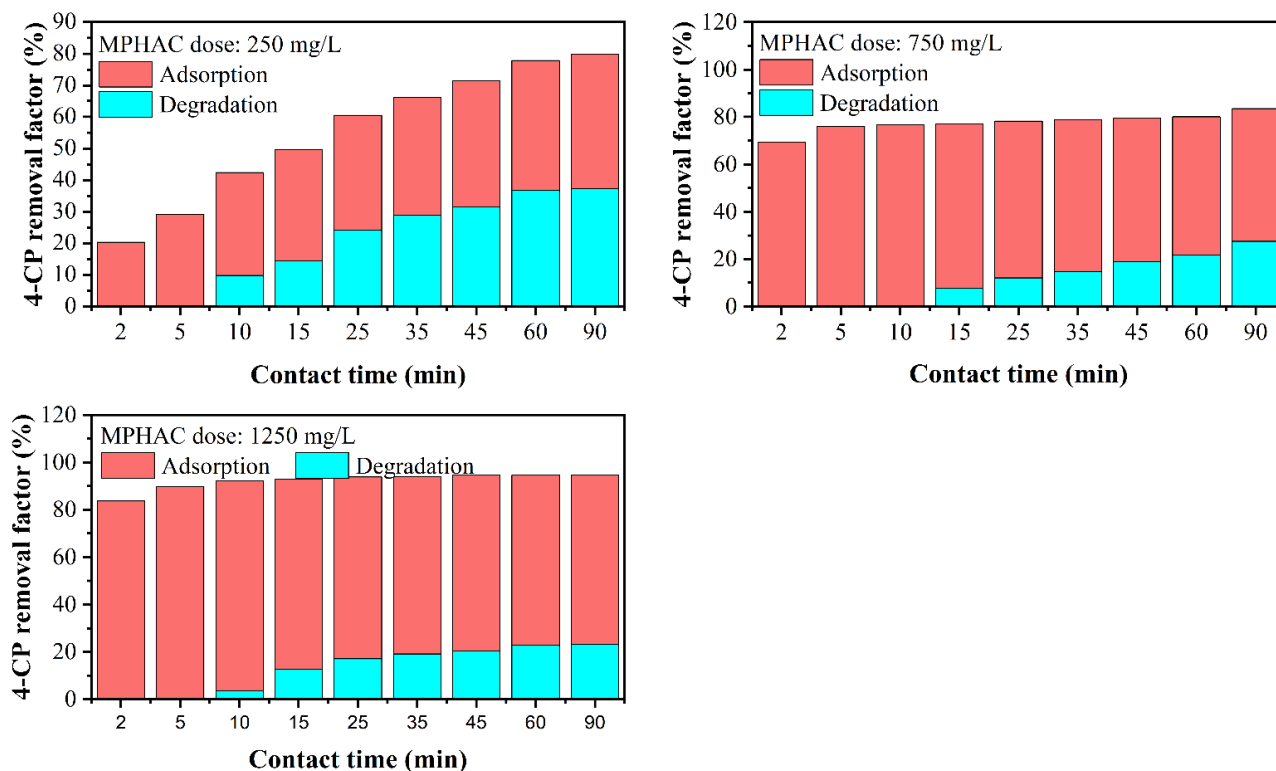


Figure 5. Effect of MPHAC dose on 4-CP removal factor by the MPHAC/PS system (initial 4-CP concentration: 100 mg/L; PS dose: 150 mg/L; and a solution pH of 5).

3.3.3. Effect of PS Dose on 4-CP Adsorption and Degradation

The dose of PS plays an important role for the production of sulfate radicals and the subsequent degradation of 4-CP. In order to determine the role of PS in 4-CP removal using the MPHAC/PS system, different doses of PS ranging from 50 to 350 mg/L were investigated (Figure 6). The results showed that 4-CP removal factor increased with increasing the PS dose (i.e., 92.5%, 94.72%, 97.9%, and 99.5% for the PS doses 50, 150, 250 and 350 mg/L, respectively, after 90 min).

As shown in Figure 6, at low doses of PS, the adsorption process plays a major role in removing 4-CP by the MPHAC/PS system. This can be explained by the fact that at low doses of PS, sufficient sulfate radicals are not produced resulting in low 4-CP degradation. This is obvious from the figure corresponding to 50 mg/L of PS dose. Moreover, by increasing the dose of PS from 50 to 350 mg/L, the degradation rate of 4-CP is enhanced, surpassing the adsorption one and inducing a higher 4-CP removal. This is due to the increase of sulfate radicals produced by the activation of PS at the catalyst surface [40]. Similar results were obtained by Zhou et al. [44], who claimed an improvement of the removal efficiency of 4-CP and a reduction of the required time to completely remove 4-CP when the concentration of the oxidant in magnetic biochar and the PS system was increased from 5 mM to 10 mM.

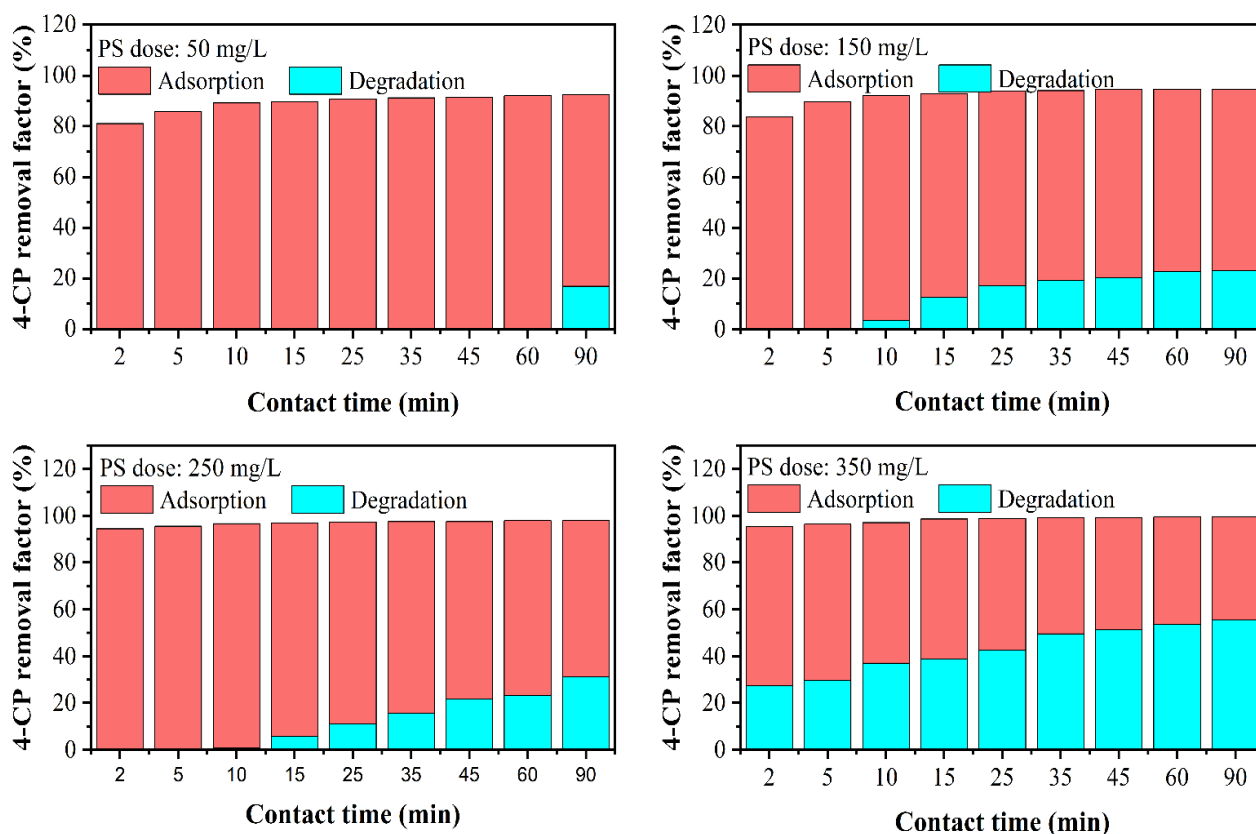


Figure 6. Effect of PS dose on 4-CP removal factor by the MPHAC/PS system (initial 4-CP concentration: 100 mg/L; MPHAC dose: 1250 mg/L; and a solution pH of 5).

3.3.4. Effect of 4-CP Initial Concentration on 4-CP Adsorption and Degradation

In addition to the initial pH of the solution, MPHAC dose and PS dose, the initial concentration of 4-CP is also important to take into account for a more efficient removal by the MPHAC/PS system. Figure 7 shows the effect of the initial 4-CP concentration on both its adsorption and degradation by the MPHAC/PS system.

As illustrated, the removal of 4-CP decreased with an increase of the initial 4-CP concentration. This is attributed to several reasons: (i) by increasing the initial 4-CP concentration from 100 to 250 mg/L, the amount of PS and catalyst is maintained constant and the ability of the MPHAC/PS system to adsorb and degrade 4-CP decreases; (ii) the competition between PS and 4-CP for placement on the catalyst surface increases with increased initial 4-CP concentration [42]; and (iii) at higher concentrations of 4-CP, it is possible to produce reaction by products (e.g., phenol, hydroquinone, benzoquinone and malonic acid, as will be explained later on), which also use sulfate radicals for their reactions and reduce 4-CP degradation [26]. Pang et al. [45] also observed a decrease of the removal efficiency of 2,4-dichlorophenol with the increase of its initial concentration. From Figure 7, it can also be seen that the increase of the initial concentration of 4-CP results in a reduction of the adsorption process with an increase of the degradation process. In fact, many of the active sites of the MPHAC are filled with 4-CP molecules as the 4-CP initial concentration increases; then, the relative portion of the adsorption process is reduced, thus the additional 4-CP molecules react with sulfate radicals, increasing the degradation process.

From all the above performed experiments, optimum operating parameters permitting a high removal of 4-CP can be determined. The highest 4-CP removal factor, 99.5%, was registered for an initial 4-CP concentration of 100 mg/L, a MPHAC dose of 1250 mg/L, PS dose of 350 mg/L, and a solution pH of 5 for 60 min contact reaction time. Pang et al. [45] studied the influence of the initial 2,4-dichlorophenol (2,4-DCP) concentration on

the degradation efficiency of 2,4-DCP by means of PS activation using magnetic graphene oxide, and observed a decrease of the 2,4-DCP removal efficiency from 100% to 40% with the increase of the concentration of 2,4-DCP from 10 to 80 mg/L.

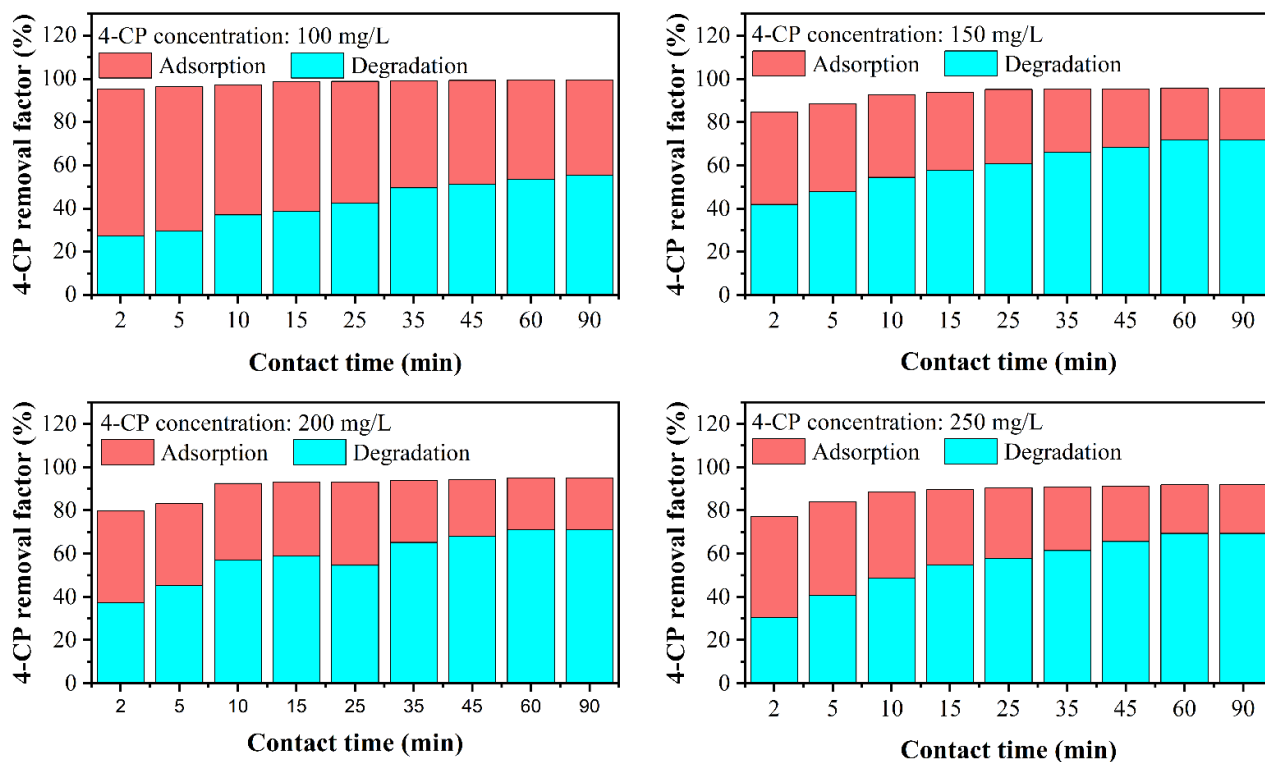


Figure 7. Effect of 4-CP concentration on 4-CP removal by the MPHAC/PS system (MPHAC dose: 1250 mg/L; PS dose: 350 mg/L; and a solution pH of 5).

3.4. Reusability of MPHAC

Reuse of catalysts is an important factor to take into consideration for their practical application. The reusability of the MPHAC was assessed through five adsorption–desorption cycles. Desorption cycle was carried out using 5 mL of acetonitrile/methanol (1/1, *v/v*), vibrated under 180 rpm for 2 h at room temperature. The adsorbent was subsequently filtered and dried overnight for subsequent use. Figure 8 shows the removal factor of 4-CP by the MPHAC/PS system used in five consecutive cycles under the defined optimum conditions (i.e., initial 4-CP concentration: 100 mg/L, MPHAC dose: 1250 mg/L, PS dose: 350 mg/L, with a solution pH of 5, and a contact reaction time of 60 min). As can be seen, the 4-CP removal factor was gradually decreased for each progressive number of cycles (i.e., 99.3%, 98.4%, 97.0%, 93.2% and 89.5%, for the cycle 1, 2, 3, 4 and 5, respectively). This decline of the 4-CP removal factor of the MPHAC/PS system is due to the reduction of both adsorption and degradation processes.

As can be seen from Figure 8, the used catalyst exhibits good stability and high efficiency towards 4-CP removal even after five cycles. This indicates its high reusability and economic viability. The slight decrease of the 4-CP removal factor observed after five cycles (<10%) can be due to the blockage of the active sites of the catalyst by intermediate products in the solution (e.g., phenol, hydroquinone, benzoquinone, malonic acid, as will be detailed in the following section), therefore hindering the binding of 4-CP molecules to the surface of the catalyst and reducing the removal of 4-CP through the adsorption process [44]. In addition, as reported by Gan et al. [46], the reduction of 4-CP removal efficiency can be attributed partly to the oxidation of divalent iron ions, which in turn reduces the production of sulfate radicals and the degradation of 4-CP.

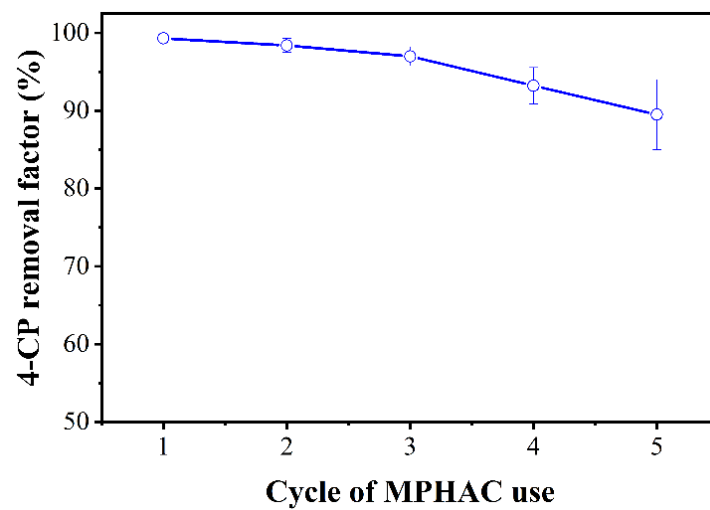


Figure 8. Reusability of MPHAC for 4-CP removal by the MPHAC/PS system (initial 4-CP concentration: 100 mg/L; MPHAC dose: 1250 mg/L; PS dose: 350 mg/L; a solution pH of 5, and a contact time of 60 min).

3.5. Possible Mechanism and Pathway of 4-CP Removal by MPHAC/PS System

In heterogeneous systems, the mechanisms of reaction are normally more complicated than homogenous systems since the reactions are catalyst surface-limiting. In addition, the chemical reactions could occur on the heterogeneous surface of iron oxides and in the homogeneous bulk solution, and also influence the iron leaching to the bulk solution [2]. Figure 9 illustrates the possible cooperation mechanism for 4-CP removal based on the simultaneous adsorption and degradation processes in the MPHAC/PS system.

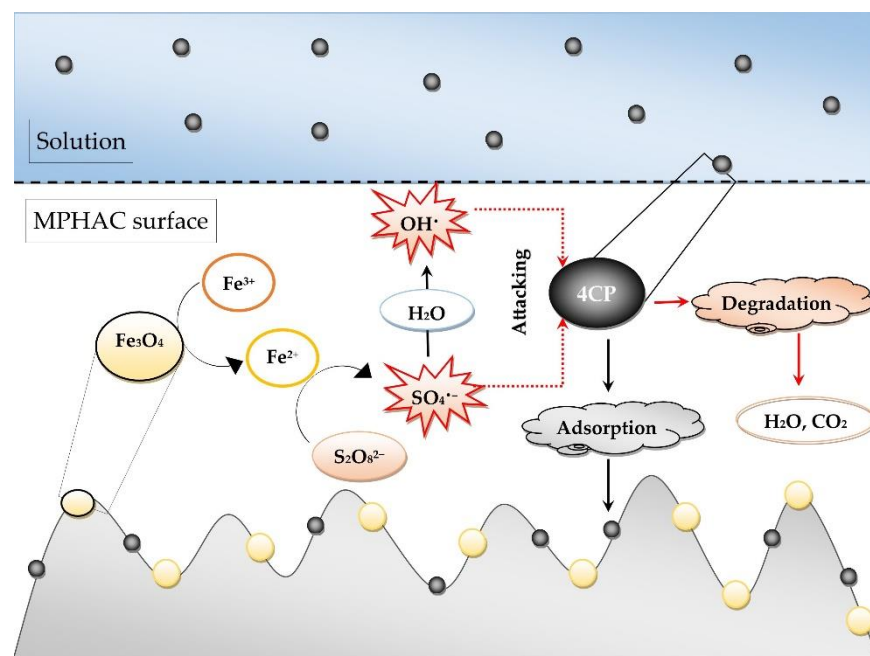


Figure 9. Simultaneous adsorption and degradation of 4-CP by the MPHAC/PS system for 4-CP removal from contaminated aqueous solutions.

During adsorption and degradation of 4-CP by the MPHAC/PS system, two mechanisms were involved, including (i) the adsorption 4-CP molecule by MPHAC grains, and (ii) the degradation of 4-CP molecules by the produced free activated radicals. For the

first mechanism, the 4-CP molecules are adsorbed on the surface of the MPHAC rains and removed from the solution without changing their structure. In the case of the second mechanism, the degradation process leads to the breakdown of the 4-CP molecule structure. In this case, the Fe_3O_4 particles present on the surface of the catalyst induce the production of iron ions, which according to Equation (1), play an important role for the enhanced activation of PS and the formation of $\text{SO}_4^{\bullet-}$ radicals. In addition, the produced $\text{SO}_4^{\bullet-}$ radicals can react with water molecules, according to Equation (8), and generate active $\bullet\text{OH}$ radicals, which, together with $\text{SO}_4^{\bullet-}$ radicals, play an important role in the 4-CP degradation [47].



The produced sulfate and hydroxyl radicals react with 4-CP molecules inducing their degradation and formation of H_2O and CO_2 after the formation of a series of intermediate compounds, as schematized in Figure 10. As illustrated in this figure, the oxidative degradation of 4-CP leads to the formation of phenol via the reduction of 4-CP by iron ions on the surface of MPHAC [48]. In addition, due to the large amount of the generated $\text{SO}_4^{\bullet-}$ and $\bullet\text{OH}$ radicals, 4-CP may be attacked by the mentioned radicals during the degradation process to produce phenol and also hydroquinone [49]. This may be due to the fact that the energy of the carbon–chloride bond is lower than that of the carbon–oxygen bond, so the first broken bands are those of carbon–chloride, resulting in the release of Cl^- ions [14]. In addition, $\text{SO}_4^{\bullet-}$ and $\bullet\text{OH}$ radicals would attack the C–C bond of benzoquinone, which was decayed to malonic acid [50]. Finally, the malonic acid was oxidized into CO_2 and H_2O with the action of activated radicals [48].

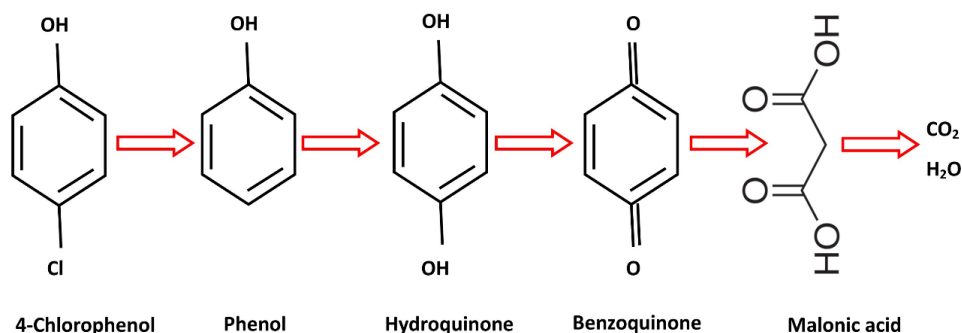


Figure 10. Possible pathway of 4-CP removal by the MPHAC/PS system.

4. Conclusions

The catalyst, magnetized activated carbon (MPHAC), was successfully synthesized, and its simultaneous use with persulfate (PS) through the MPHAC/PS system increased the removal efficiency of 4-CP from water, thanks to the simultaneous adsorption and degradation processes. The initial solution pH, catalyst dose and PS dose exerted significant effects on the 4-CP removal. The obtained optimal conditions (MPHAC dose: 1250 mg/L, PS dose: 350 mg/L, and a solution pH of 5) for an initial 4-CP concentration of 100 mg/L and a contact time of 60 min, resulted in a 99.5% removal factor of 4-CP from water. The catalyst has a high stability, and after five successive cycles, the 4-CP removal efficiency decreased by only 10%. The possible mechanism and pathway, in addition to how adsorption and degradation processes affect the removal of 4-CP from the MPHAC/PS system, investigated possible intermediaries created during the reaction. Given the above explanations and the excellent removal of 4-CP from water by the MPHAC/PS system, it can be concluded that the MPHAC/PS system is a type of Fenton-like process that can be used to remove organic compounds, such as phenolic compounds.

Author Contributions: The individual contributions are provided as follows. Methodology and investigation, S.H. and E.T.; Writing-original draft preparation, S.H., E.T. and M.M.A.; Conceptualization, A.F., E.T. and M.K.; Supervision and project administration, A.F. and E.T.; Writing-review and editing, A.F. and M.K. All authors have read and agreed to the published version of the manuscript.

Funding: Present study funded by the Isfahan University of Medical Sciences (IUMS) of Iran, under Project No. 298169.

Institutional Review Board Statement: Not applicable.

Informed Consent Statement: Not applicable.

Data Availability Statement: Not applicable.

Acknowledgments: This study was financially supported by the Isfahan University of Medical Sciences (IUMS) of Iran, under Project No. 298169, with ethical code #IR.MUI.RESEARCH.REC.1398.636.

Conflicts of Interest: The authors declare that they have no known competing financial interests or personal relationships that could have appeared to influence the work reported in this paper.

References

1. Madannejad, S.; Rashidi, A.; Sadeghassani, S.; Shemirani, F.; Ghasemy, E. Removal of 4-chlorophenol from water using different carbon nanostructures: A comparison study. *J. Mol. Liq.* **2018**, *249*, 877–885. [\[CrossRef\]](#)
2. Hadi, S.; Taheri, E.; Amin, M.M.; Fatehizadeh, A.; Lima, E.C. Fabrication of activated carbon from pomegranate husk by dual consecutive chemical activation for 4-chlorophenol adsorption. *Environ. Sci. Pollut. Res.* **2020**, *28*, 13919–13930. [\[CrossRef\]](#) [\[PubMed\]](#)
3. Olaniran, A.O.; Igbinsola, E.O. Chlorophenols and other related derivatives of environmental concern: Properties, distribution and microbial degradation processes. *Chemosphere* **2011**, *83*, 1297–1306. [\[CrossRef\]](#) [\[PubMed\]](#)
4. Czaplicka, M. Sources and transformations of chlorophenols in the natural environment. *Sci. Total Environ.* **2004**, *322*, 21–39. [\[CrossRef\]](#)
5. Fatehizadeh, A.; Zare, M.R.; Van Ginkel, S.W.; Taheri, E.; Amin, M.M.; Rafiei, N.; Mahdavi, M. Methyl tertiary-butyl ether adsorption by bioactivated carbon from aqueous solution: Kinetics, isotherm and artificial neural network modeling. *Desalin. Water Treat.* **2019**, *154*, 254–267. [\[CrossRef\]](#)
6. Amin, M.M.; Taheri, E.; Fatehizadeh, A.; Rezakazemi, M.; Aminabhavi, T.M. Anaerobic membrane bioreactor for the production of bioH₂: Electron flow, fouling modeling and kinetic study. *Chem. Eng. J.* **2021**, *426*, 130716. [\[CrossRef\]](#)
7. Amin, M.M.; Taheri, E.; Ghasemian, M.; Puad, N.I.M.; Dehdashti, B.; Fatehizadeh, A. Proposal of upgrading Isfahan north wastewater treatment plant: An adsorption/bio-oxidation process with emphasis on excess sludge reduction and nutrient removal. *J. Clean. Prod.* **2020**, *255*, 120247. [\[CrossRef\]](#)
8. Amin, M.M.; Bina, B.; Taheri, E.; Fatehizadeh, A.; Ghasemian, M. Stoichiometry evaluation of biohydrogen production from various carbohydrates. *Environ. Sci. Pollut. Res.* **2016**, *23*, 20915–20921. [\[CrossRef\]](#)
9. Hadi, S.; Taheri, E.; Amin, M.M.; Fatehizadeh, A.; Gardas, R.L. Empirical modeling and kinetic study of methylene blue removal from synthetic wastewater by activation of persulfate with heterogeneous Fenton-like process. *J. Mol. Liq.* **2021**, *328*, 115408. [\[CrossRef\]](#)
10. Khajeh, M.; Amin, M.M.; Taheri, E.; Fatehizadeh, A.; McKay, G. Influence of co-existing cations and anions on removal of direct red 89 dye from synthetic wastewater by hydrodynamic cavitation process: An empirical modeling. *Ultrason. Sonochemistry* **2020**, *67*, 105133. [\[CrossRef\]](#)
11. Hadi, S.; Taheri, E.; Amin, M.M.; Fatehizadeh, A.; Aminabhavi, T.M. Advanced oxidation of 4-chlorophenol via combined pulsed light and sulfate radicals methods: Effect of co-existing anions. *J. Environ. Manag.* **2021**, *291*, 112595. [\[CrossRef\]](#)
12. Rajaei, F.; Taheri, E.; Hadi, S.; Fatehizadeh, A.; Amin, M.M.; Rafei, N.; Fadaei, S.; Aminabhavi, T.M. Enhanced removal of humic acid from aqueous solution by combined alternating current electrocoagulation and sulfate radical. *Environ. Pollut.* **2021**, *277*, 116632. [\[CrossRef\]](#)
13. Khajeh, M.; Amin, M.M.; Fatehizadeh, A.; Aminabhavi, T.M. Synergetic degradation of atenolol by hydrodynamic cavitation coupled with sodium persulfate as zero-waste discharge process: Effect of coexisting anions. *Chem. Eng. J.* **2021**, *416*, 129163. [\[CrossRef\]](#)
14. Hadi, S.; Taheri, E.; Amin, M.M.; Fatehizadeh, A.; Aminabhavi, T.M. Synergistic degradation of 4-chlorophenol by persulfate and oxalic acid mixture with heterogeneous Fenton like system for wastewater treatment: Adaptive neuro-fuzzy inference systems modeling. *J. Environ. Manag.* **2020**, *268*, 110678. [\[CrossRef\]](#)
15. Xu, X.-R.; Li, X.-Z. Degradation of azo dye Orange G in aqueous solutions by persulfate with ferrous ion. *Sep. Purif. Technol.* **2010**, *72*, 105–111. [\[CrossRef\]](#)
16. Jonidi Jafari, A.; Kakavandi, B.; Jaafarzadeh, N.; Rezaei Kalantary, R.; Ahmadi, M.; Akbar Babaei, A. Fenton-like catalytic oxidation of tetracycline by AC@Fe₃O₄ as a heterogeneous persulfate activator: Adsorption and degradation studies. *J. Ind. Eng. Chem.* **2017**, *45*, 323–333. [\[CrossRef\]](#)

17. Li, X.; Zhou, M.; Pan, Y. Enhanced degradation of 2,4-dichlorophenoxyacetic acid by pre-magnetization Fe-C activated persulfate: Influential factors, mechanism and degradation pathway. *J. Hazard. Mater.* **2018**, *353*, 454–465. [[CrossRef](#)]
18. Chen, H.; Yang, Y.; Wei, J.; Xu, J.; Li, J.; Wang, P.; Xu, J.; Han, Y.; Jin, H.; Jin, D.; et al. Cobalt ferrites/activated carbon: Synthesis, magnetic separation and catalysis for potassium hydrogen persulfate. *Mater. Sci. Eng. B* **2019**, *249*, 114420. [[CrossRef](#)]
19. Hamdaoui, O.; Naffrechoux, E. Adsorption kinetics of 4-chlorophenol onto granular activated carbon in the presence of high frequency ultrasound. *Ultrason. Sonochemistry* **2009**, *16*, 15–22. [[CrossRef](#)]
20. Kuleyin, A. Removal of phenol and 4-chlorophenol by surfactant-modified natural zeolite. *J. Hazard. Mater.* **2007**, *144*, 307–315. [[CrossRef](#)]
21. Papaioannou, E.H.; Mitrouli, S.T.; Patsios, S.I.; Kazakli, M.; Karabelas, A.J. Valorization of pomegranate husk—Integration of extraction with nanofiltration for concentrated polyphenols recovery. *J. Environ. Chem. Eng.* **2020**, *8*, 103951. [[CrossRef](#)]
22. Pathak, P.D.; Mandavgane, S.A.; Kulkarni, B.D. Valorization of pomegranate peels: A biorefinery approach. *Waste Biomass Valorization* **2017**, *8*, 1127–1137. [[CrossRef](#)]
23. Akhtar, S.; Ismail, T.; Fraternali, D.; Sestili, P. Pomegranate peel and peel extracts: Chemistry and food features. *Food Chem.* **2015**, *174*, 417–425. [[CrossRef](#)]
24. Sood, A.; Gupta, M. Extraction process optimization for bioactive compounds in pomegranate peel. *Food Biosci.* **2015**, *12*, 100–106. [[CrossRef](#)]
25. Singh, B.; Singh, J.P.; Kaur, A.; Singh, N. Antimicrobial potential of pomegranate peel: A review. *Int. J. Food Sci. Technol.* **2019**, *54*, 959–965. [[CrossRef](#)]
26. Sun, K.; Li, J.; Peng, H.; Feng, E.; Ma, G.; Lei, Z. Promising nitrogen-doped porous nanosheets carbon derived from pomegranate husk as advanced electrode materials for supercapacitors. *Ionics* **2017**, *23*, 985–996. [[CrossRef](#)]
27. Lima, D.R.; Hosseini-Bandegharai, A.; Thue, P.S.; Lima, E.C.; de Albuquerque, Y.R.T.; dos Reis, G.S.; Umpierrez, C.S.; Dias, S.L.P.; Tran, H.N. Efficient acetaminophen removal from water and hospital effluents treatment by activated carbons derived from Brazil nutshells. *Colloids Surf. A* **2019**, *583*, 123966. [[CrossRef](#)]
28. Hadi, S.; Taheri, E.; Amin, M.M.; Fatehizadeh, A.; Aminabhavi, T.M. Adsorption of 4-chlorophenol by magnetized activated carbon from pomegranate husk using dual stage chemical activation. *Chemosphere* **2020**, *270*, 128623. [[CrossRef](#)]
29. Ben-Ali, S. Application of Raw and Modified Pomegranate Peel for Wastewater Treatment: A Literature Overview and Analysis. *Int. J. Chem. Eng.* **2021**, *2021*, 8840907. [[CrossRef](#)]
30. Do, M.H.; Phan, N.H.; Nguyen, T.D.; Pham, T.T.S.; Nguyen, V.K.; Vu, T.T.T.; Nguyen, T.K.P. Activated carbon/Fe₃O₄ nanoparticle composite: Fabrication, methyl orange removal and regeneration by hydrogen peroxide. *Chemosphere* **2011**, *85*, 1269–1276. [[CrossRef](#)] [[PubMed](#)]
31. Khaledi, K.; Valdes Labrada, G.M.; Soltan, J.; Predicala, B.; Nemati, M. Adsorptive removal of tetracycline and lincomycin from contaminated water using magnetized activated carbon. *J. Environ. Chem. Eng.* **2021**, *9*, 105998. [[CrossRef](#)]
32. Sing, K.S.; Everett, D.; Haul, R.; Moscou, L.; Pierotti, R.; Rouquerol, J.; Siemieniewska, T. Reporting physisorption data for gas/solid systems with special reference to the determination of surface area and porosity (Recommendations 1984). *Pure Appl. Chem.* **1985**, *57*, 603–619. [[CrossRef](#)]
33. Wang, C.; Jiang, H.-L.; Yuan, N.; Pei, Y.; Yan, Z. Tuning the adsorptive properties of drinking water treatment residue via oxygen-limited heat treatment for environmental recycle. *Chem. Eng. J.* **2016**, *284*, 571–581. [[CrossRef](#)]
34. Tran, H.N.; Wang, Y.-F.; You, S.-J.; Chao, H.-P. Insights into the mechanism of cationic dye adsorption on activated charcoal: The importance of π - π interactions. *Process Saf. Environ. Prot.* **2017**, *107*, 168–180. [[CrossRef](#)]
35. Čerović, L.S.; Milonjić, S.K.; Todorović, M.B.; Trtanj, M.I.; Pogozhev, Y.S.; Blagoveschenskii, Y.; Levashov, E.A. Point of zero charge of different carbides. *Colloids Surf. A* **2007**, *297*, 1–6. [[CrossRef](#)]
36. Su, H.; Dou, X.; Xu, D.; Feng, L.; Liu, Y.; Du, Z.; Zhang, L. Fe₀-loaded superfine powdered activated carbon prepared by ball milling for synergistic adsorption and persulfate activation to remove aqueous carbamazepine. *Chemosphere* **2022**, *293*, 133665. [[CrossRef](#)]
37. Rahmani, Z.; Kermani, M.; Gholami, M.; Jafari, A.J.; Mahmoodi, N.M. Effectiveness of photochemical and sonochemical processes in degradation of Basic Violet 16 (BV16) dye from aqueous solutions. *Iran. J. Environ. Health Sci. Eng.* **2012**, *9*, 1–7. [[CrossRef](#)]
38. Forouzesh, M.; Ebadi, A.; Aghaeinejad-Meybodi, A. Degradation of metronidazole antibiotic in aqueous medium using activated carbon as a persulfate activator. *Sep. Purif. Technol.* **2019**, *210*, 145–151. [[CrossRef](#)]
39. Liu, C.S.; Shih, K.; Sun, C.X.; Wang, F. Oxidative degradation of propachlor by ferrous and copper ion activated persulfate. *Sci. Total Environ.* **2012**, *416*, 507–512. [[CrossRef](#)]
40. Chen, J.; Yu, X.; Li, C.; Tang, X.; Sun, Y. Removal of tetracycline via the synergistic effect of biochar adsorption and enhanced activation of persulfate. *Chem. Eng. J.* **2020**, *382*, 122916. [[CrossRef](#)]
41. Dehghan, S.; Kakavandi, B.; Kalantary, R.R. Heterogeneous sonocatalytic degradation of amoxicillin using ZnO@Fe₃O₄ magnetic nanocomposite: Influential factors, reusability and mechanisms. *J. Mol. Liq.* **2018**, *264*, 98–109. [[CrossRef](#)]
42. Zhou, R.; Zhao, J.; Shen, N.; Ma, T.; Su, Y.; Ren, H. Efficient degradation of 2,4-dichlorophenol in aqueous solution by peroxy-monosulfate activated with magnetic spinel FeCo₂O₄ nanoparticles. *Chemosphere* **2018**, *197*, 670–679. [[CrossRef](#)] [[PubMed](#)]
43. Rao, L.; Yang, Y.; Liu, X.; Huang, Y.; Chen, M.; Yao, Y.; Wang, W. Heterogeneous activation of persulfate by supporting ferric oxalate onto activated carbon fibers for organic contaminants removal. *Mater. Res. Bull.* **2020**, *130*, 110919. [[CrossRef](#)]

44. Zhou, H.; Zhu, X.; Chen, B. Magnetic biochar supported α -MnO₂ nanorod for adsorption enhanced degradation of 4-chlorophenol via activation of peroxydisulfate. *Sci. Total Environ.* **2020**, *724*, 138278. [[CrossRef](#)] [[PubMed](#)]
45. Pang, Y.; Zhou, Y.; Luo, K.; Zhang, Z.; Yue, R.; Li, X.; Lei, M. Activation of persulfate by stability-enhanced magnetic graphene oxide for the removal of 2,4-dichlorophenol. *Sci. Total Environ.* **2020**, *707*, 135656. [[CrossRef](#)]
46. Gan, Q.; Hou, H.; Liang, S.; Qiu, J.; Tao, S.; Yang, L.; Yu, W.; Xiao, K.; Liu, B.; Hu, J.; et al. Sludge-derived biochar with multivalent iron as an efficient Fenton catalyst for degradation of 4-Chlorophenol. *Sci. Total Environ.* **2020**, *725*, 138299. [[CrossRef](#)] [[PubMed](#)]
47. Chanikya, P.; Nidheesh, P.V.; Syam Babu, D.; Gopinath, A.; Suresh Kumar, M. Treatment of dyeing wastewater by combined sulfate radical based electrochemical advanced oxidation and electrocoagulation processes. *Sep. Purif. Technol.* **2021**, *254*, 117570. [[CrossRef](#)]
48. Li, S.; Tang, J.; Liu, Q.; Liu, X.; Gao, B. A novel stabilized carbon-coated nZVI as heterogeneous persulfate catalyst for enhanced degradation of 4-chlorophenol. *Environ. Int.* **2020**, *138*, 105639. [[CrossRef](#)]
49. Xu, M.; Chen, Y.; Qin, J.; Feng, Y.; Li, W.; Chen, W.; Zhu, J.; Li, H.; Bian, Z. Unveiling the Role of Defects on Oxygen Activation and Photodegradation of Organic Pollutants. *Environ. Sci. Technol.* **2018**, *52*, 13879–13886. [[CrossRef](#)]
50. Gao, Y.; Wang, Q.; Ji, G.; Li, A. Degradation of antibiotic pollutants by persulfate activated with various carbon materials. *Chem. Eng. J.* **2022**, *429*, 132387. [[CrossRef](#)]